

# A Fully Quaternion-Valued Capon Beamformer Based on Crossed-Dipole Arrays

Xiang Lan and Wei Liu  
Communications Research Group  
Department of Electronic and Electrical Engineering  
University of Sheffield, UK

**Abstract**—Quaternion models have been developed for both direction of arrival estimation and beamforming based on crossed-dipole arrays in the past. However, for almost all the models, especially for adaptive beamforming, the desired signal is still complex-valued and one example is the quaternion-Capon beamformer. However, since the complex-valued desired signal only has two components, while there are four components in a quaternion, only two components of the quaternion-valued beamformer output are used and the remaining two are simply removed. This leads to significant redundancy in its implementation. In this work, we consider a quaternion-valued desired signal and develop a full quaternion-valued Capon beamformer, which has a better performance and a much lower complexity and is shown to be more robust against array pointing errors.

**Keywords** — quaternion model, crossed-dipole, Capon beamformer, vector sensor array.

## I. INTRODUCTION

Electromagnetic (EM) vector sensor arrays can track the direction of arrival (DOA) of impinging signals as well as their polarization. A crossed-dipole sensor array, firstly introduced in [1] for adaptive beamforming, works by processing the received signals with a long polarization vector. Based on such a model, the beamforming problem is studied in detail in terms of output signal-to-interference-plus-noise ratio (SINR) [2]. In [3], [4], further detailed analysis was performed showing that the output SINR is affected by DOA and polarization differences.

Since there are four components for each vector sensor output in a crossed-dipole array, a quaternion model instead of long vectors has been adopted in the past for both adaptive beamforming and direction of arrival (DOA) estimation [5]–[9]. In [10], the well-known Capon beamformer was extended to the quaternion domain and a quaternion-valued Capon (Q-Capon) beamformer was proposed with the corresponding optimum solution derived.

However, in most of the beamforming studies, the signal of interest (SOI) is still complex-valued, i.e. with only two components: in-phase (I) and quadrature (Q). Since the output of a quaternion-valued beamformer is also quaternion-valued, only two components of the quaternion are used to recover the SOI, which leads to redundancy in both calculation and data storage. However, with the development of quaternion-valued wireless communications [11]–[13], it is very likely that in the future we will have quaternion-valued signals as the SOI, where two traditional complex-valued signals with different polarisations arrive at the array with the same DOA.

In such a case, a full quaternion-valued array model is needed to compactly represent the four-component desired signal and also make sure the four components of the quaternion-valued output of the beamformer are fully utilised. In this work, we develop such a model and propose a new quaternion-valued Capon beamformer, where both its input and output are quaternion-valued.

This paper is structured as follows. The full quaternion-valued array model is introduced in Section II and the proposed quaternion-valued Capon beamformer is developed in Section III. Simulation results are presented in IV, and conclusions are drawn in Section V.

## II. QUATERNION MODEL FOR ARRAY PROCESSING

A quaternion is constructed by four components [14], [15], with one real part and three imaginary parts, which is defined as  $q = q_a + iq_b + jq_c + kq_d$ , where  $i, j, k$  are three different imaginary units and  $q_a, q_b, q_c, q_d$  are real-valued. The multiplication principle among such units is

$$i^2 = j^2 = k^2 = ijk = -1, \quad (1)$$

and

$$ij = -ji = k, ki = -ik = j, jk = -kj = i \quad (2)$$

The conjugate  $q^*$  of  $q$  is  $q^* = q_a - iq_b - jq_c - kq_d$ .

A quaternion number can be conveniently denoted as a combination of two complex numbers  $q = c_1 + ic_2$ , where the complex number  $c_1 = q_a + jq_c$  and  $c_2 = q_b + jq_d$ . We will use this form later to represent our quaternion-valued signal of interest.

Consider a uniform linear array with  $N$  crossed-dipole sensors, as shown in Fig. 1, where the adjacent vector sensor spacing  $d$  equals half wavelength, and the two components of each crossed-dipole are parallel to  $x$ - and  $y$ -axes, respectively. A quaternion-valued narrowband signal  $s_0(t)$  impinges upon the vector sensor array among other  $M$  uncorrelated quaternion-valued interfering signals  $\{s_m(t)\}_{m=1}^M$ , with background noise  $n(t)$ .  $s_0(t)$  can be decomposed into

$$s_0(t) = s_{01}(t) + is_{02}(t), \quad (3)$$

where  $s_{01}(t)$  and  $s_{02}(t)$  are two complex-valued sub-signals with the same DOA but different polarizations.

Assume that all signals are ellipse-polarized. The parameters, including DOA and polarization of the  $m$ -th signal are denoted by  $(\theta_m, \phi_m, \gamma_{m1}, \eta_{m1})$  for the first sub-signal and

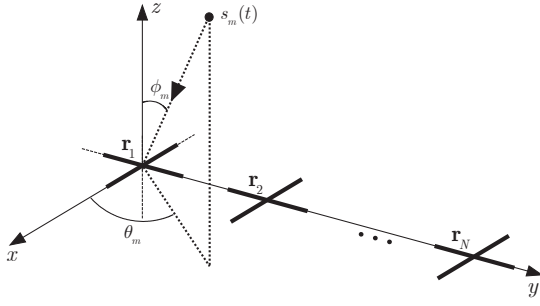


Fig. 1. A crossed-dipole linear array with  $N$  vector sensors.

$(\theta_m, \phi_m, \gamma_{m2}, \eta_{m2})$  for the second sub-signal. Each crossed-dipole sensor receives signals both in the  $x$  and  $y$  sub-arrays.

For signal  $s_m(t)$ , the corresponding received signals at the  $x$  and  $y$  sub-arrays are respectively given by [16]:

$$\begin{aligned} \mathbf{x}(t) &= \mathbf{a}_{m1} p_{xm1} s_{m1}(t) + \mathbf{a}_{m2} p_{xm2} s_{m2}(t) \\ \mathbf{y}(t) &= \mathbf{a}_{m1} p_{ym1} s_{m1}(t) + \mathbf{a}_{m2} p_{ym2} s_{m2}(t) \end{aligned} \quad (4)$$

where  $\mathbf{x}(t)$  represents the received part in the  $x$ -sub-array,  $\mathbf{y}(t)$  represents the part in the  $y$ -sub-array, and  $(p_{xm1}, p_{ym1})$  and  $(p_{xm2}, p_{ym2})$  are the polarizations of the two complex sub-signals in  $x$  and  $y$  directions, respectively, which are given by [17],

$$\begin{aligned} p_{xm1} &= -\cos \gamma_{m1} \\ p_{ym1} &= \cos \phi_m \sin \gamma_{m1} e^{j\eta_{m1}} \\ p_{xm2} &= -\cos \gamma_{m2} \\ p_{ym2} &= \cos \phi_m \sin \gamma_{m2} e^{j\eta_{m2}}, \quad \text{when } \theta_m = \frac{\pi}{2} \end{aligned} \quad (5)$$

Note that  $\mathbf{a}_{m1}$  and  $\mathbf{a}_{m2}$  are the steering vectors for the two sub-signals, which are equal to each other since the two sub-signals share the same DOA  $(\theta_m, \phi_m)$ .

$$\begin{aligned} \mathbf{a}_{m1} &= [1 \ e^{-j\frac{2\pi \sin \theta_m \sin \phi_m}{\lambda}} \dots e^{-j\frac{(N-1)2\pi \sin \theta_m \sin \phi_m}{\lambda}}]^T \\ \mathbf{a}_{m2} &= [1 \ e^{-j\frac{2\pi \sin \theta_m \sin \phi_m}{\lambda}} \dots e^{-j\frac{(N-1)2\pi \sin \theta_m \sin \phi_m}{\lambda}}]^T \end{aligned} \quad (6)$$

A quaternion model can be constructed by combining the two parts as below:

$$\begin{aligned} \mathbf{q}_m(t) &= \mathbf{x}(t) + i\mathbf{y}(t) \\ &= \mathbf{a}_{m1}(p_{xm1} + ip_{ym1})s_{m1}(t) \\ &\quad + \mathbf{a}_{m2}(p_{xm2} + ip_{ym2})s_{m2}(t) \\ &= \mathbf{b}_{m1}s_{m1}(t) + \mathbf{b}_{m2}s_{m2}(t) \end{aligned} \quad (7)$$

where  $\{\mathbf{b}_{m1}, \mathbf{b}_{m2}\} \in \mathbb{H}^{N \times 1}$  can be considered as the composite quaternion-valued steering vector. Combining all source signals and the noise together, the result is given by:

$$\mathbf{q}(t) = \sum_{m=0}^M (\mathbf{b}_{m1}s_{m1}(t) + \mathbf{b}_{m2}s_{m2}(t)) + \mathbf{n}_q(t) \quad (9)$$

where  $\mathbf{n}_q(t) = \mathbf{n}_x(t) + i\mathbf{n}_y(t)$  is the quaternion-valued noise vector consisting of the two sub-array noise vectors  $\mathbf{n}_x(t)$  and  $\mathbf{n}_y(t)$ .

### III. FULL QUATERNION CAPON BEAMFORMER

#### A. The Full Q-Capon Beamformer

To recover the SOI among interfering signals and noise, the basic idea is to keep a unity response to the SOI at the beamformer output and then reduce the power/variance of the output as much as possible [18], [19]. The key to construct such a Capon beamformer in the quaternion domain is to design an appropriate constraint to make sure the quaternion-valued SOI can pass through the beamformer with the desired unity response.

Again note that the quaternion-valued SOI can be expressed as a combination of two complex sub-signals. To construct such a constraint, one choice is to make sure the first complex sub-signal of the SOI pass through the beamformer and appear in the real and  $j$  components of the beamformer output, while the second complex sub-signal appear in the  $i$  and  $k$  components of the beamformer output. Then, with a quaternion-valued weight vector  $\mathbf{w}$ , the constraint can be formulated as

$$\mathbf{w}^H \mathbf{C} = \mathbf{f} \quad (10)$$

where  $\{\}^H$  is the Hermitian transpose (combination of the quaternion-valued conjugate and transpose operation),  $\mathbf{C} = [\mathbf{b}_{01} \ \mathbf{b}_{02}]$ , and  $\mathbf{f} = [1 \ i]$ .

With this constraint, the beamformer output  $z(t)$  is given by

$$\begin{aligned} z(t) &= \mathbf{w}^H \mathbf{q}(t) \\ &= \underbrace{s_{01}(t) + is_{02}(t)}_{s_0(t)} + \mathbf{w}^H \mathbf{n}_q(t) \\ &\quad + \sum_{m=1}^M \mathbf{w}^H [\mathbf{b}_{m1}s_{m1}(t) + \mathbf{b}_{m2}s_{m2}(t)] \end{aligned} \quad (11)$$

Clearly, the quaternion-valued SOI has been preserved at the output with the desired unity response.

Now, the full-quaternion Capon (full Q-Capon) beamformer can be formulated as

$$\min \mathbf{w}^H \mathbf{R} \mathbf{w} \quad \text{subject to } \mathbf{w}^H \mathbf{C} = \mathbf{f} \quad (12)$$

where

$$\mathbf{R} = E\{\mathbf{q}(t)\mathbf{q}^H(t)\}. \quad (13)$$

Applying the Lagrange multiplier method, we have

$$l(\mathbf{w}, \boldsymbol{\lambda}) = \mathbf{w}^H \mathbf{R} \mathbf{w} + (\mathbf{w}^H \mathbf{C} - \mathbf{f}) \boldsymbol{\lambda}^H + \boldsymbol{\lambda} (\mathbf{C}^H \mathbf{w} - \mathbf{f}^H) \quad (14)$$

where  $\boldsymbol{\lambda}$  is a quaternion-valued vector.

The minimum can be obtained by setting the gradient of (14) with respect to  $\mathbf{w}^*$  equal to a zero vector [20]. It is given by

$$\nabla_{\mathbf{w}^*} l(\mathbf{w}, \boldsymbol{\lambda}) = \frac{1}{2} \mathbf{R} \mathbf{w} + \frac{1}{2} \mathbf{C} \boldsymbol{\lambda}^H = \mathbf{0} \quad (15)$$

Considering all the constraints above, we obtain the optimum weight vector  $\mathbf{w}_{opt}$  as follows

$$\mathbf{w}_{opt} = \mathbf{R}^{-1} \mathbf{C} (\mathbf{C}^H \mathbf{R}^{-1} \mathbf{C})^{-1} \mathbf{f}^H. \quad (16)$$

A detailed derivation for the quaternion-valued optimum weight vector can be found at the Appendix.

In the next subsection, we give a brief analysis to show that by this optimum weight vector, the interference part at the beamformer output  $z(t)$  in (11) has been suppressed effectively.

### B. Interference Suppression

Expanding the covariance matrix, we have

$$\mathbf{R} = E\{\mathbf{q}(t)\mathbf{q}^H(t)\} = \mathbf{R}_{i+n} + \sigma_1^2 \mathbf{b}_{01} \mathbf{b}_{01}^H + \sigma_2^2 \mathbf{b}_{02} \mathbf{b}_{02}^H \quad (17)$$

where  $\sigma_1^2, \sigma_2^2$  are the power of the two sub-signals of SOI and  $\mathbf{R}_{i+n}$  denotes the covariance matrix of interferences plus noise. Using the Sherman-Morrison formula, we then have

$$\mathbf{w}_{opt} = \mathbf{R}_{i+n}^{-1} \mathbf{C} \boldsymbol{\beta} \quad (18)$$

where  $\boldsymbol{\beta} = (\mathbf{C}^H \mathbf{R}_{i+n} \mathbf{C})^{-1} \mathbf{f}^H \in \mathbb{H}^{2 \times 1}$  is a quaternion vector.

Applying left eigendecomposition for quaternion matrix [21]–[23],

$$\mathbf{R}_{i+n} = \sum_{n=1}^N \alpha_n \mathbf{u}_n \mathbf{u}_n^H \quad (19)$$

with  $\alpha_1 \geq \dots \geq \alpha_{M-2} > \alpha_{M-1} = \dots = \alpha_N = 2\sigma_0^2 \in \mathbb{R}$ , where  $2\sigma_0^2$  denotes the noise power.

With sufficiently high interference to noise ratio (INR), the inverse of  $\mathbf{R}_{i+n}$  can be approximated by

$$\mathbf{R}_{i+n}^{-1} \approx \sum_{n=M+1}^N \frac{1}{2\sigma_0^2} \mathbf{u}_n \mathbf{u}_n^H \quad (20)$$

Then, we have

$$\mathbf{w}_{opt} = \sum_{n=M+1}^N \frac{1}{2\sigma_0^2} \mathbf{u}_n \mathbf{u}_n^H \mathbf{C} \boldsymbol{\beta} = \sum_{n=M+1}^N \mathbf{u}_n \rho_n \quad (21)$$

where  $\rho_n$  is a quaternion-valued constant. Clearly,  $\mathbf{w}_{opt}$  is the right linear combination of  $\{u_{M+1}, u_{M+2}, \dots, u_N\}$ , and  $\mathbf{w} \in \text{span}_R\{u_{M+1}, u_{M+2}, \dots, u_N\}$ .

For those  $M$  interfering signals, their quaternion steering vectors belong to the space right-spanned by the related  $M$  eigenvectors, i.e.  $\mathbf{b}_{m1}, \mathbf{b}_{m2} \in \text{span}_R\{u_1, u_2, \dots, u_M\}$ . As a result,

$$\mathbf{w}_{opt}^H \mathbf{b}_{m1} \approx 0, \mathbf{w}_{opt}^H \mathbf{b}_{m2} \approx 0, m = 1, 4, \dots, M \quad (22)$$

which shows that the beamformer has eliminated the interferences effectively.

### C. Complexity Analysis

In this section, we make a comparison of the computation complexity between the Q-Capon beamformer in [10] and our proposed full Q-Capon beamformer. To deal with a quaternion-valued signal, the Q-Capon beamformer has to process the two complex sub-signals separately to recover the desired signal completely, which means we need to apply the beamformer twice for a quaternion-valued SOI. However, for the full Q-Capon beamformer, the SOI is recovered directly by applying the beamformer once.

For the Q-Capon beamformer, the weight vector is calculated by  $\mathbf{w} = \mathbf{R}^{-1} \mathbf{a}_0 (\mathbf{a}_0^H \mathbf{R}^{-1} \mathbf{a}_0)^{-1}$ , where  $\mathbf{a}_0$  is the steering vector for the complex-valued SOI. As an example, we

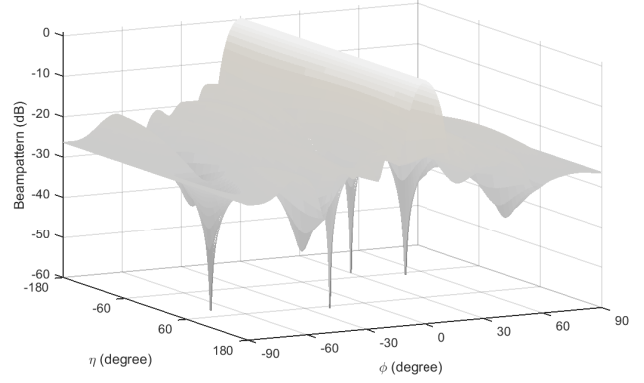


Fig. 2. The resultant beam pattern with  $\theta = 90^\circ$  and  $\gamma = 60^\circ$ .

use Gaussian elimination to calculate the matrix inversion  $\mathbf{R}^{-1}$  and  $\frac{1}{3}(N^3 - N)$  quaternion-valued multiplications are needed, equivalent to  $\frac{16}{3}(N^3 - N)$  real-valued multiplications. Additionally,  $\mathbf{R}^{-1} \mathbf{a}_0$  requires  $16N^2$  real-valued multiplications, while  $16(N^2 + N)$  real multiplications are needed for  $(\mathbf{a}_0^H \mathbf{R}^{-1} \mathbf{a}_0)^{-1}$ . In total,  $\frac{16}{3}N^3 + 32N^2 + \frac{80}{3}N$  real multiplications are needed. When processing a quaternion-valued signal, this number will be doubled and the total number of real multiplications becomes  $\frac{32}{3}N^3 + 64N^2 + \frac{160}{3}N$ .

For the proposed full Q-Capon beamformer, in addition to calculating  $\mathbf{R}^{-1}$ ,  $32N^2$  real multiplications are required to calculate  $\mathbf{R}^{-1} \mathbf{C}$  and  $32M^2 + 32M + 96$  real multiplications for  $(\mathbf{C}^H \mathbf{R}^{-1} \mathbf{C}_0)^{-1} \mathbf{f}$ . In total, the number of real-valued multiplications is  $\frac{16}{3}M^3 + 64M^2 + \frac{272}{3}M + 96$ , which is roughly half of that of the Q-Capon beamformer.

## IV. SIMULATIONS RESULTS

In our simulations, we consider 10 pairs of cross-dipoles with half wave-length spacing. All signals are assumed to arrive from the same plane of  $\theta = 90^\circ$  and all interferences have the same polarization parameter  $\gamma = 60^\circ$ . For the SOI, the two sub-signals are set to  $(90^\circ, 1.5^\circ, 90^\circ, 45^\circ)$  and  $(90^\circ, 1.5^\circ, 0^\circ, 0^\circ)$ , with interferences coming from  $(90^\circ, 30^\circ, 60^\circ, -80^\circ)$ ,  $(90^\circ, -70^\circ, 60^\circ, 30^\circ)$ ,  $(90^\circ, -20^\circ, 60^\circ, 70^\circ)$ ,  $(90^\circ, 50^\circ, 60^\circ, -50^\circ)$ , respectively. The background noise is zero-mean quaternion-valued Gaussian. The power of SOI and all interfering signals are set equal and SNR (INR) is 20dB.

Fig. 2 shows the resultant 3-D beam pattern by the proposed beamformer, where the interfering signals from  $(\phi, \eta) = (30^\circ, -80^\circ)$ ,  $(-70^\circ, 30^\circ)$ ,  $(-20^\circ, 70^\circ)$  and  $(50^\circ, -50^\circ)$  have all been effectively suppressed.

In the following, the output SINR performance of the two Capon beamformers (full Q-Capon and Q-Capon) is studied with the DOA and polarization  $(90^\circ, 1.5^\circ, 90^\circ, 45^\circ)$  and  $(90^\circ, 1.5^\circ, 0^\circ, 0^\circ)$  for SOI and  $(90^\circ, 30^\circ, 60^\circ, -80^\circ)$ ,  $(90^\circ, -70^\circ, 60^\circ, 30^\circ)$ ,  $(90^\circ, -20^\circ, 60^\circ, 70^\circ)$ ,  $(90^\circ, 50^\circ, 60^\circ, -50^\circ)$  for interferences. Again, we have set SNR=INR=20dB. All results are obtained by averaging 1000 Monte-Carlo trials.

Fig. 3 shows the output SINR performance versus SNR with 100 snapshots, where the solid-line is for the optimal

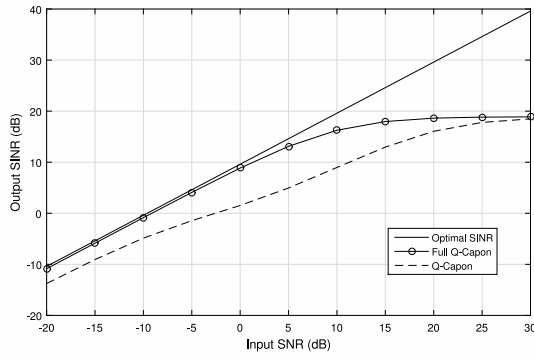


Fig. 3. Output SINR versus input SNR (snapshots number 100).

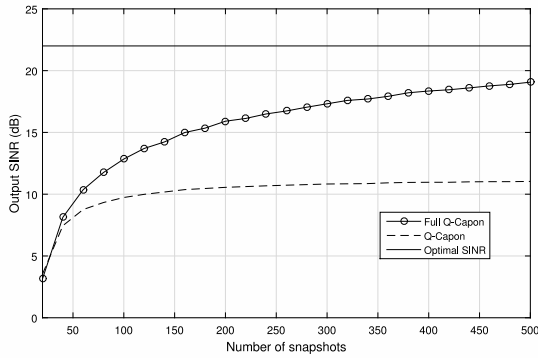


Fig. 4. Output SINR versus snapshot number with SNR=SIR=15dB and 1° error.

beamformer with infinite number of snapshots. For most of the input SNR range, in particular the lower range, the proposed full Q-Capon beamformer has a better performance than the Q-Capon beamformer. For very high input SNR values, these two beamformers have a very similar performance.

Next, we investigate their performance in the presence of DOA and polarization errors. The output SINR with respect to the number of snapshots is shown in Fig. 4 in the presence of 1° error for the SOI, where the real DOA and polarization parameters are (91°, 2.5°, 91°, 46°) and (91°, 2.5°, 1°, 1°). It can be seen that the full Q-Capon beamformer has achieved a much higher output SINR than the Q-Capon beamformer, and this gap increases with the increase of snapshot number. Fig. 5 shows a similar trend in the presence of a 5° error. Overall, we can see that the proposed full Q-Capon beamformer is more robust against array pointing errors.

## V. CONCLUSIONS

In this paper, a full quaternion model has been developed for adaptive beamforming based on crossed-dipole arrays, with a new full quaternion Capon beamformer proposed. Different from previous studies in quaternion-valued adaptive beamforming, we have considered a quaternion-valued desired signal, given the recent development in quaternion-valued

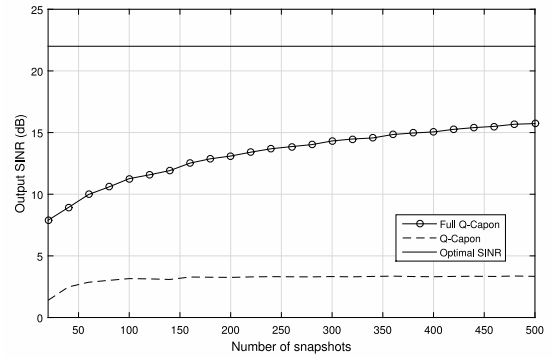


Fig. 5. Output SINR versus snapshot number with SNR=SIR=15dB and 5° error.

wireless communications research. The proposed beamformer has a better performance and a much lower computational complexity than a previously proposed Q-Capon beamformer and is also shown to be more robust against array pointing errors, as demonstrated by computer simulations.

## APPENDIX

The gradient of a quaternion vector  $\mathbf{u} = \mathbf{w}^H \mathbf{C} \boldsymbol{\lambda}^H$  with respect to  $\mathbf{w}^*$  can be calculated as below:

$$\nabla_{\mathbf{w}^*} \mathbf{u} = [\nabla_{w_1^*} \mathbf{u} \quad \nabla_{w_2^*} \mathbf{u} \quad \dots \quad \nabla_{w_N^*} \mathbf{u}]^T \quad (23)$$

where  $w_n$ ,  $n = 1, 2, \dots, N$  is the  $n$ -th quaternion-valued coefficient of the beamformer. Then,

$$\nabla_{w_1^*} \mathbf{u} = \frac{1}{4} (\nabla_{w_{1a}} \mathbf{u} + \nabla_{w_{1b}} \mathbf{u} i + \nabla_{w_{1c}} \mathbf{u} j + \nabla_{w_{1d}} \mathbf{u} k) \quad (24)$$

where

$$w_1^* = w_{1a} - w_{1b}i - w_{1c}j - w_{1d}k \quad (25)$$

Since  $w_{1a}$  is real-valued, with the chain rule [20], we have

$$\begin{aligned} \nabla_{w_{1a}} \mathbf{u} &= \nabla_{w_{1a}} (\mathbf{w}^H) \mathbf{C} \boldsymbol{\lambda}^H + \mathbf{w}^H \nabla_{w_{1a}} (\mathbf{C} \boldsymbol{\lambda}^H) \\ &= [1 \quad 0 \quad 0 \quad \dots \quad 0] \mathbf{C} \boldsymbol{\lambda}^H \end{aligned} \quad (26)$$

Similarly,

$$\begin{aligned} \nabla_{w_{1b}} \mathbf{u} &= [-i \quad 0 \quad 0 \quad \dots \quad 0] \mathbf{C} \boldsymbol{\lambda}^H \\ \nabla_{w_{1c}} \mathbf{u} &= [-j \quad 0 \quad 0 \quad \dots \quad 0] \mathbf{C} \boldsymbol{\lambda}^H \\ \nabla_{w_{1d}} \mathbf{u} &= [-k \quad 0 \quad 0 \quad \dots \quad 0] \mathbf{C} \boldsymbol{\lambda}^H \end{aligned}$$

Hence,

$$\nabla_{w_1^*} \mathbf{u} = \frac{1}{4} (4 \text{Real}(\mathbf{C} \boldsymbol{\lambda}^H)_1) = \text{Real}(\mathbf{C} \boldsymbol{\lambda}^H)_1, \quad (27)$$

where the subscript  $\{ \}_1$  in the last item means taking the first entry of the vector.

Finally,

$$\nabla_{\mathbf{w}^*} \mathbf{u} = \text{Real}(\mathbf{C} \boldsymbol{\lambda}^H) \quad (28)$$

The gradient of the quaternion vector  $\mathbf{v} = \boldsymbol{\lambda} \mathbf{C}^H \mathbf{w}$  with respect to  $\mathbf{w}^*$  can be calculated in the same way:

$$\begin{aligned} \nabla_{w_{1a}} \mathbf{v} &= \boldsymbol{\lambda} \mathbf{C}^H \nabla_{w_{1a}} \mathbf{w} + \nabla_{w_{1a}} (\boldsymbol{\lambda} \mathbf{C}^H) \mathbf{w} \\ &= \boldsymbol{\lambda} \mathbf{C}^H [1 \quad 0 \quad 0 \quad \dots \quad 0]^T \end{aligned} \quad (29)$$

Similarly,

$$\begin{aligned}\nabla_{w_{1b}} \mathbf{v} &= \boldsymbol{\lambda} \mathbf{C}^H [i \ 0 \ 0 \ \dots \ 0]^T \\ \nabla_{w_{1c}} \mathbf{v} &= \boldsymbol{\lambda} \mathbf{C}^H [j \ 0 \ 0 \ \dots \ 0]^T \\ \nabla_{w_{1d}} \mathbf{v} &= \boldsymbol{\lambda} \mathbf{C}^H [k \ 0 \ 0 \ \dots \ 0]^T\end{aligned}\quad (30)$$

Thus, the gradient can be expressed as

$$\nabla_{w_1^*} \mathbf{v} = -\frac{1}{2}(\mathbf{C}\boldsymbol{\lambda}^H)^* \quad (31)$$

Finally,

$$\nabla_{w^*} \mathbf{v} = -\frac{1}{2}(\mathbf{C}\boldsymbol{\lambda}^H)^* \quad (32)$$

The gradient of  $c_w = \mathbf{w}^H \mathbf{R} \mathbf{w}$  can be calculated as follows.

$$\nabla_{w^*} c_w = [\nabla_{w_1^*} c_w \quad \nabla_{w_2^*} c_w \quad \dots \quad \nabla_{w_n^*} c_w]^T \quad (33)$$

$$\nabla_{w_1^*} c_w = \frac{1}{4}(\nabla_{w_{1a}} c_w + \nabla_{w_{1b}} c_w i + \nabla_{w_{1c}} c_w j + \nabla_{w_{1d}} c_w k) \quad (34)$$

Now we calculate the gradient of  $c_w$  with respect to the four components of  $w_1$ .

$$\begin{aligned}\nabla_{w_{1a}} c_w &= \nabla_{w_{1a}} (\mathbf{w}^H \mathbf{R}) \mathbf{w} + \mathbf{w}^H \mathbf{R} \nabla_{w_{1a}} \mathbf{w} \\ &= [1 \ 0 \ 0 \ \dots \ 0] \mathbf{R} \mathbf{w} \\ &\quad + \mathbf{w}^H \mathbf{R} [1 \ 0 \ 0 \ \dots \ 0]^T\end{aligned}\quad (35)$$

The other three components are,

$$\begin{aligned}\nabla_{w_{1b}} c_w &= [-i \ 0 \ 0 \ \dots \ 0] \mathbf{R} \mathbf{w} \\ &\quad + \mathbf{w}^H \mathbf{R} [i \ 0 \ 0 \ \dots \ 0]^T \\ \nabla_{w_{1c}} c_w &= [-j \ 0 \ 0 \ \dots \ 0] \mathbf{R} \mathbf{w} \\ &\quad + \mathbf{w}^H \mathbf{R} [j \ 0 \ 0 \ \dots \ 0]^T \\ \nabla_{w_{1d}} c_w &= [-k \ 0 \ 0 \ \dots \ 0] \mathbf{R} \mathbf{w} \\ &\quad + \mathbf{w}^H \mathbf{R} [k \ 0 \ 0 \ \dots \ 0]^T\end{aligned}$$

Hence,

$$\nabla_{w_1^*} c_w = \text{Real}(\mathbf{R} \mathbf{w})_1 - \frac{1}{2}(\mathbf{R} \mathbf{w})_1^* = \frac{1}{2}(\mathbf{R} \mathbf{w})_1 \quad (36)$$

Finally,

$$\nabla_{w^*} c_w = \frac{1}{2} \mathbf{R} \mathbf{w} \quad (37)$$

Combining (28), (32) and (37), with (14), we have

$$\nabla_{w^*} l(\mathbf{w}, \boldsymbol{\lambda}) = \frac{1}{2}(\mathbf{R} \mathbf{w} + \mathbf{C} \boldsymbol{\lambda}^H) = \mathbf{0} \quad (38)$$

Further,

$$\mathbf{w} = -2\mathbf{R}^{-1} \mathbf{C} \boldsymbol{\lambda}^H \quad (39)$$

Substituting (39) into (10),

$$\boldsymbol{\lambda} = -\frac{1}{2} \mathbf{f}(\mathbf{C}^H \mathbf{R}^{-1} \mathbf{C})^{-1} \quad (40)$$

Finally,

$$\mathbf{w} = \mathbf{R}^{-1} \mathbf{C}(\mathbf{C}^H \mathbf{R}^{-1} \mathbf{C})^{-1} \mathbf{f}^H \quad (41)$$

## REFERENCES

- [1] R. Compton Jr, "On the performance of a polarization sensitive adaptive array," *IEEE Transactions on Antennas and Propagation*, vol. 29, no. 5, pp. 718–725, September 1981.
- [2] A. Nehorai, K. C. Ho, and B. T. G. Tan, "Minimum-noise-variance beamformer with an electromagnetic vector sensor," *IEEE Transactions on Signal Processing*, vol. 47, no. 3, pp. 601–618, March 1999.
- [3] L. C. Godara, "Application of antenna arrays to mobile communications. ii. beam-forming and direction-of-arrival considerations," *Proceedings of the IEEE*, vol. 85, no. 8, pp. 1195–1245, August 1997.
- [4] Y. G. Xu, T. Liu, and Z. W. Liu, "Output SINR of MV beamformer with one EM vector sensor of and magnetic noise power," in *Proc. of International Conference on Signal Processing*, September 2004, pp. 419–422.
- [5] S. Miron, N. Le Bihan, and J. I. Mars, "High resolution vector-sensor array processing using quaternions," in *Proc. of IEEE Workshop on Statistical Signal Processing*, July 2005, pp. 918–923.
- [6] —, "Quaternion-music for vector-sensor array processing," *IEEE Transactions on Signal Processing*, vol. 54, no. 4, pp. 1218–1229, April 2006.
- [7] X. Gong, Y. Xu, and Z. Liu, "Quaternion ESPRIT for direction finding with a polarization sensitive array," in *Proc. of International Conference on Signal Processing*, October 2008, pp. 378–381.
- [8] J. W. Tao and W. X. Chang, "A novel combined beamformer based on hypercomplex processes," *IEEE Transactions on Aerospace and Electronic Systems*, vol. 49, no. 2, pp. 1276–1289, 2013.
- [9] X. R. Zhang, W. Liu, Y. G. Xu, and Z. W. Liu, "Quaternion-valued robust adaptive beamformer for electromagnetic vector-sensor arrays with worst-case constraint," *Signal Processing*, vol. 104, pp. 274–283, November 2014.
- [10] X. Gou, Y. Xu, Z. Liu, and X. Gong, "Quaternion-capon beamformer using crossed-dipole arrays," in *Proc. of IEEE International Symposium on Microwave, Antenna, Propagation, and EMC Technologies for Wireless Communications (MAPE)*, November 2011, pp. 34–37.
- [11] O. M. Isaeva and V. A. Sarytchev, "Quaternion presentations polarization state," in *Proc. 2nd IEEE Topical Symposium of Combined Optical-Microwave Earth and Atmosphere Sensing*, Atlanta, US, April 1995, pp. 195–196.
- [12] B. J. Wysocki and T. A. Wysocki, "On an orthogonal space-time-polarization block code," *Journal of Communications*, vol. 4, no. 1, pp. 20–25, February 2009.
- [13] W. Liu, "Antenna array signal processing for a quaternion-valued wireless communication system," in *Proc. the Benjamin Franklin Symposium on Microwave and Antenna Sub-systems (BenMAS)*, Philadelphia, US, September 2014.
- [14] W. R. Hamilton, *Elements of Quaternions*. Longmans, Green, & co., 1866.
- [15] I. Kantor, A. S. Solodovnikov, and A. Shenitzer, *Hypercomplex Numbers: an Elementary Introduction to Algebras*. New York: Springer Verlag, 1989.
- [16] X. Zhang, W. Liu, Y. Xu, and Z. Liu, "quaternion-valued robust adaptive beamformer for electromagnetic vector-sensor arrays with worst-case constraint," *Signal Processing*, vol. 104, pp. 274–283, November 2014.
- [17] M. Hawes and W. Liu, "Design of fixed beamformers based on vector-sensor arrays," *International Journal of Antennas and Propagation*, vol. 2015, April 2015.
- [18] J. Capon, "High-resolution frequency-wavenumber spectrum analysis," *Proceedings of the IEEE*, vol. 57, no. 8, pp. 1408–1418, August 1969.
- [19] O. L. Frost, III, "An algorithm for linearly constrained adaptive array processing," *Proceedings of the IEEE*, vol. 60, no. 8, pp. 926–935, August 1972.
- [20] M. D. Jiang, Y. Li, and W. Liu, "Properties of a general quaternion-valued gradient operator and its application to signal processing," *Frontiers of Information Technology & Electronic Engineering*, vol. 17, pp. 83–95, February 2016.
- [21] F. Zhang, "Quaternions and matrices of quaternions," *Linear algebra and its applications*, vol. 251, pp. 21–57, January 1997.
- [22] L. Huang and W. So, "On left eigenvalues of a quaternionic matrix," *Linear algebra and its applications*, vol. 323, no. 1, pp. 105–116, January 2001.
- [23] N. Le Bihan and J. Mars, "Singular value decomposition of quaternion matrices: a new tool for vector-sensor signal processing," *Signal processing*, vol. 84, no. 7, pp. 1177–1199, July 2004.